RESEARCH ARTICLE

Figures and figure supplements

Ciliary Hedgehog signaling regulates cell survival to build the facial midline

Shaun Abrams and Jeremy F Reiter

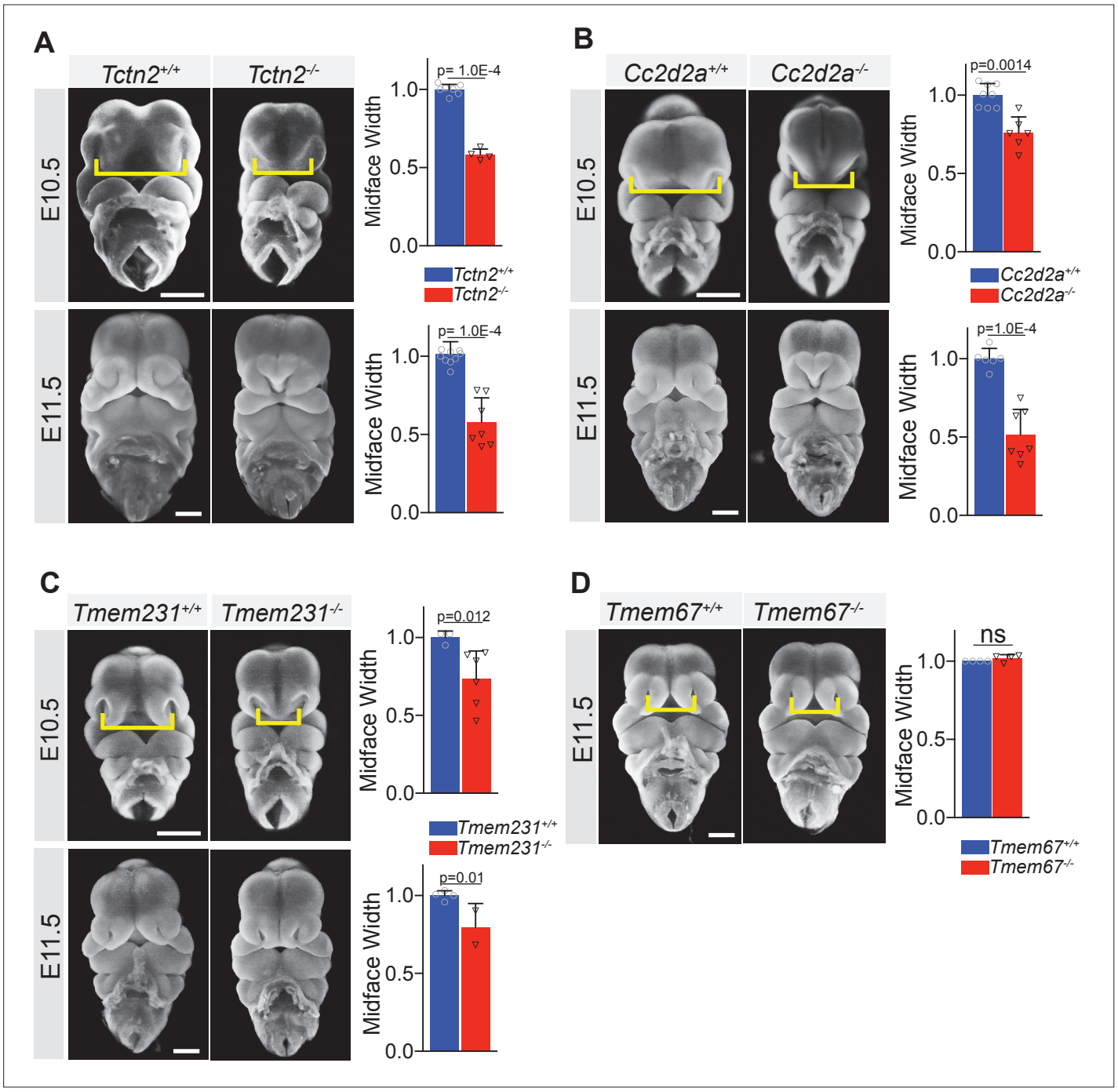

Figure 1. The ciliary Meckel syndrome (MKS) transition zone complex is essential for midline facial development. Frontal view images of *Tctn2* (**A**), *Cc2d2a* (**B**), *Tmem231* (**C**) wildtype and null embryos at embryonic day (E)10.5 and E11.5. *Tmem67* null embryos (**D**) display normal midface width at E11.5. Quantification of midface width (denoted by yellow brackets) at respective timepoints was measured via one-way ANOVA followed by Tukey's multiple comparisons test. Data are expressed as mean, and error bars represent the standard deviation (SD) with individual data points (N) representing biological replicates (biologically distinct samples). Scale bar indicates 500 μm. ns = not significant.

Figure 1- Figure Supplement 1. The ciliary MKS transition zone complex is essential for midline facial development

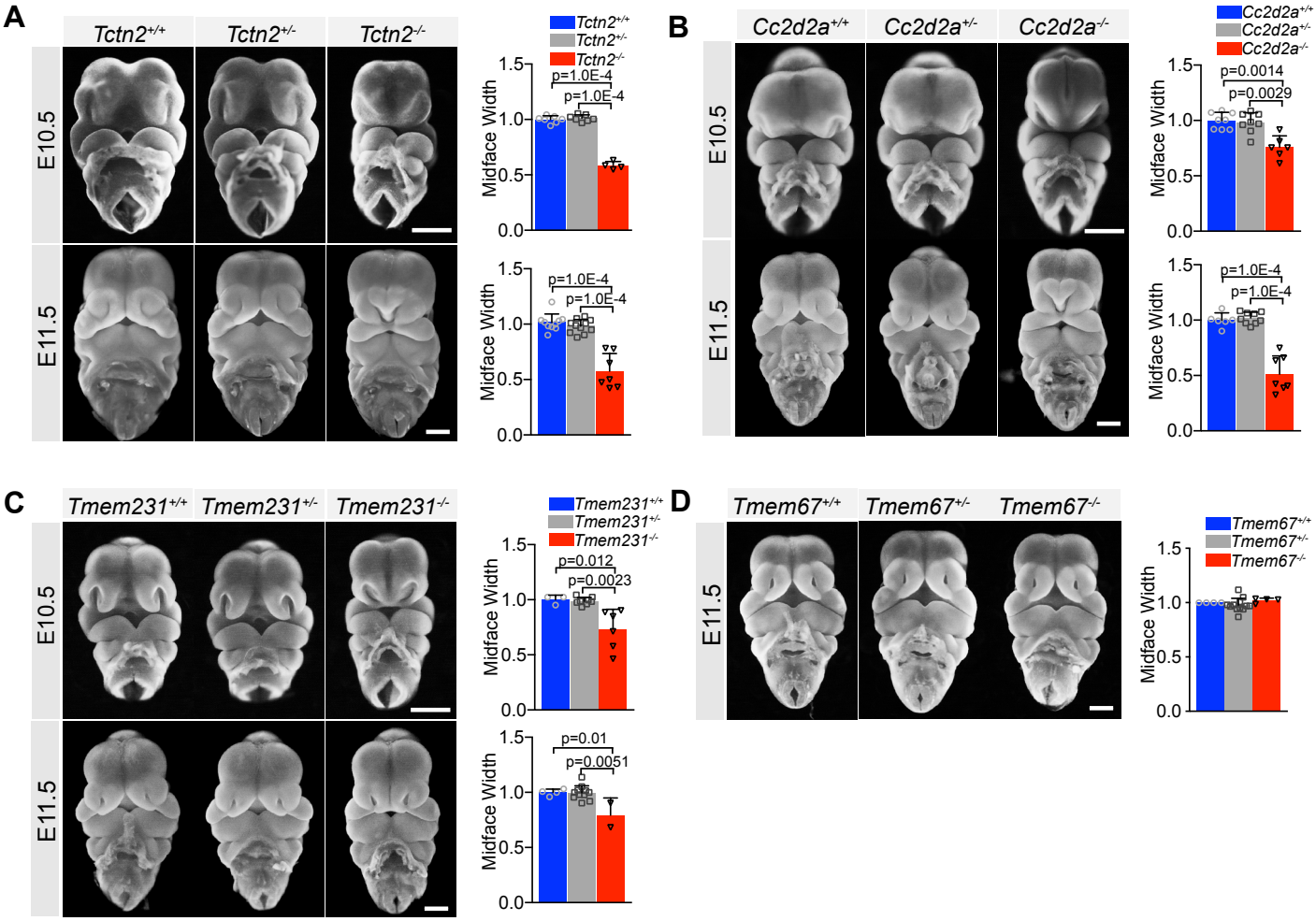

Reproduced frontal view images from Figure 1 of *Tctn2* (A), *Cc2d2a* (B), *Tmem231* (C), wildtype and null embryos at E10.5 and E11.5 with the addition of heterozygous embryos. (D) *Tmem67* null and wildtype E11.5 embryos reproduced from Figure 1 with addition of heterozygous embryos. Quantification of midface width at respective timepoints measured via one-way Anova followed by Tukey's multiple comparisons test. Error bars represent the standard deviation (SD) and each data point indicates a biological replicate (biologically distinct sample). Scale bar indicates 500μm.

Figure 1—figure supplement 1. The ciliary Meckel syndrome (MKS) transition zone complex is essential for midline facial development. Reproduced frontal view images from ***Figure 1*** of *Tctn2* (**A**), *Cc2d2a* (**B**), *Tmem231* (**C**), wildtype and null embryos at embryonic day (E)10.5 and E11.5 with the addition of heterozygous embryos. (**D**) *Tmem67* null and wildtype E11.5 embryos reproduced from ***Figure 1*** with addition of heterozygous embryos. Quantification of midface width at respective timepoints measured via one-way ANOVA followed by Tukey's multiple comparisons test. Error bars represent the standard deviation (SD) and each data point indicates a biological replicate. Scale bar indicates 500 μm.

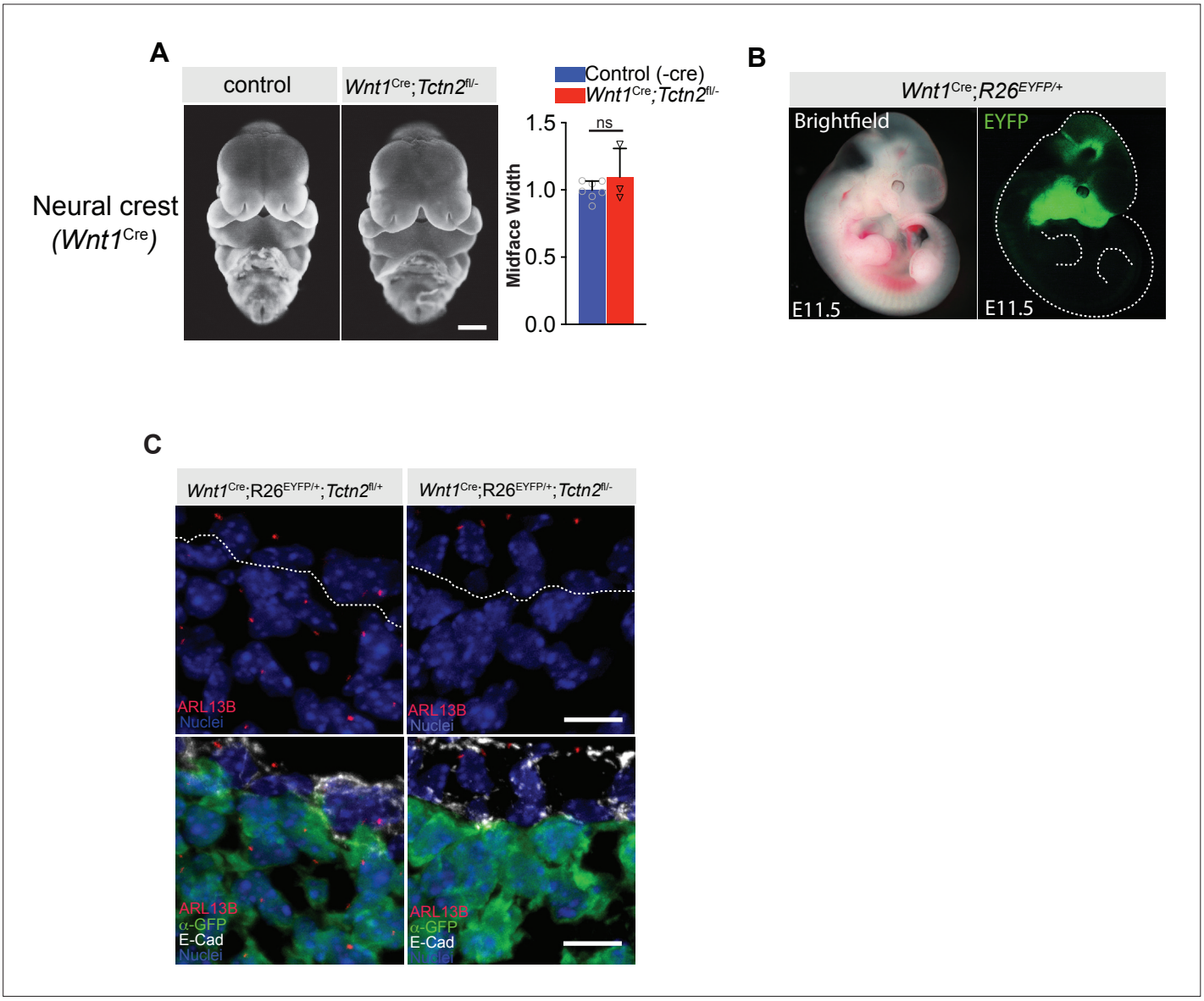

Figure 1—figure supplement 2. Removing TCTN2 in the neural crest does not result in hypotelorism. (**A**) Frontal view images of embryonic day (E)11.5 *Tctn2* control (*Tctn2*$^{lox/-}$) and neural crest deletion (*Wnt1*^{Cre};*Tctn2*$^{fl/-}$) embryos with corresponding midface width quantification. (**B**) Brightfield and fluorescent images of E11.5 *Wnt1*^{Cre};*R26*$^{EYFP/+}$ embryos show expected pattern of Cre recombination (embryo outlined with white dotted line in B). (**C**) Immunofluorescence staining of E10.5 medial nasal prominence sections for ciliary membrane protein ARL13B, GFP, and epithelial marker E-cadherin (E-Cad). Dotted white line in (**C**) represents boundary separating epithelia and neural crest mesenchyme. Quantified data in A represents the mean with error bars indicating standard deviation (SD) and each individual data point indicates a biological replicate. Student's *t* test performed for statistical analysis of (**A**), ns = not significant. Scale bars indicate 500 μm (**A**) and 10 μm (**C**).

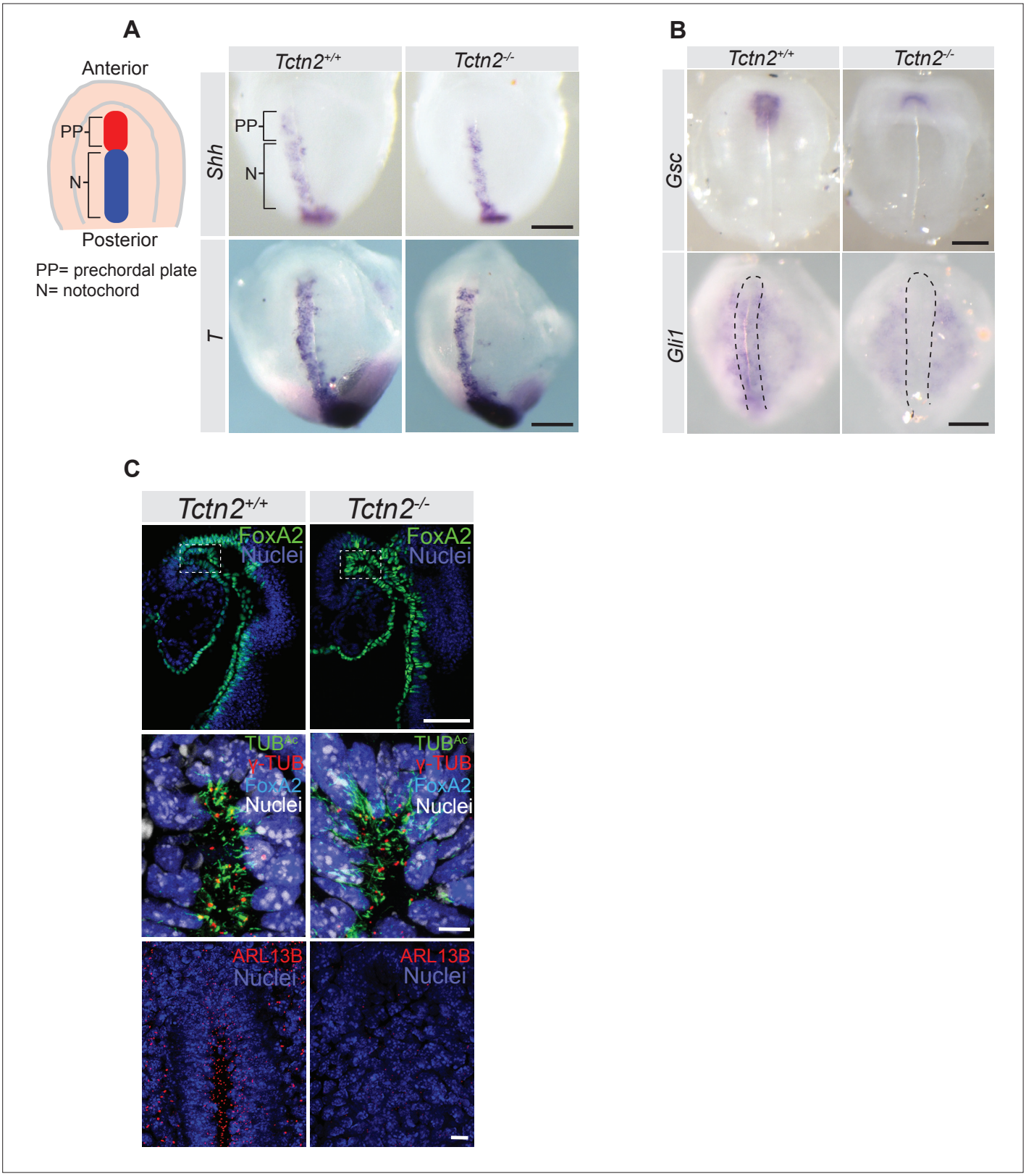

Figure 2. *Tctn2* mutants exhibit defects in prechordal plate differentiation soon after gastrulation.** (**A**) Whole mount in situ hybridization (WM-ISH) of embryonic day (E)8.0 embryos for axial mesendoderm markers *Shh* and *Shh* and *Brachyury* (*T*). (**B**) WM-ISH of E8.0 embryos for prechordal plate marker *Goosecoid* (*Gsc*) and Hedgehog (HH) pathway target *Gli1*. (**C**) Whole mount immunofluorescence staining for the cilia marker acetylated tubulin (TUB^{Ac}), basal body marker gamma tubulin (γ -TUB), and ciliary membrane protein ARL13B in E8.0 embryos. Middle panel in C is magnified region in top panel

Figure 2 continued on next page

Figure 2 continued

highlighted by dotted rectangle and rotated 90 degrees. Scale bar in A–B indicates 0.2 mm, C (top panel) is 100 μm, C (middle and bottom panels) is 10 μm.

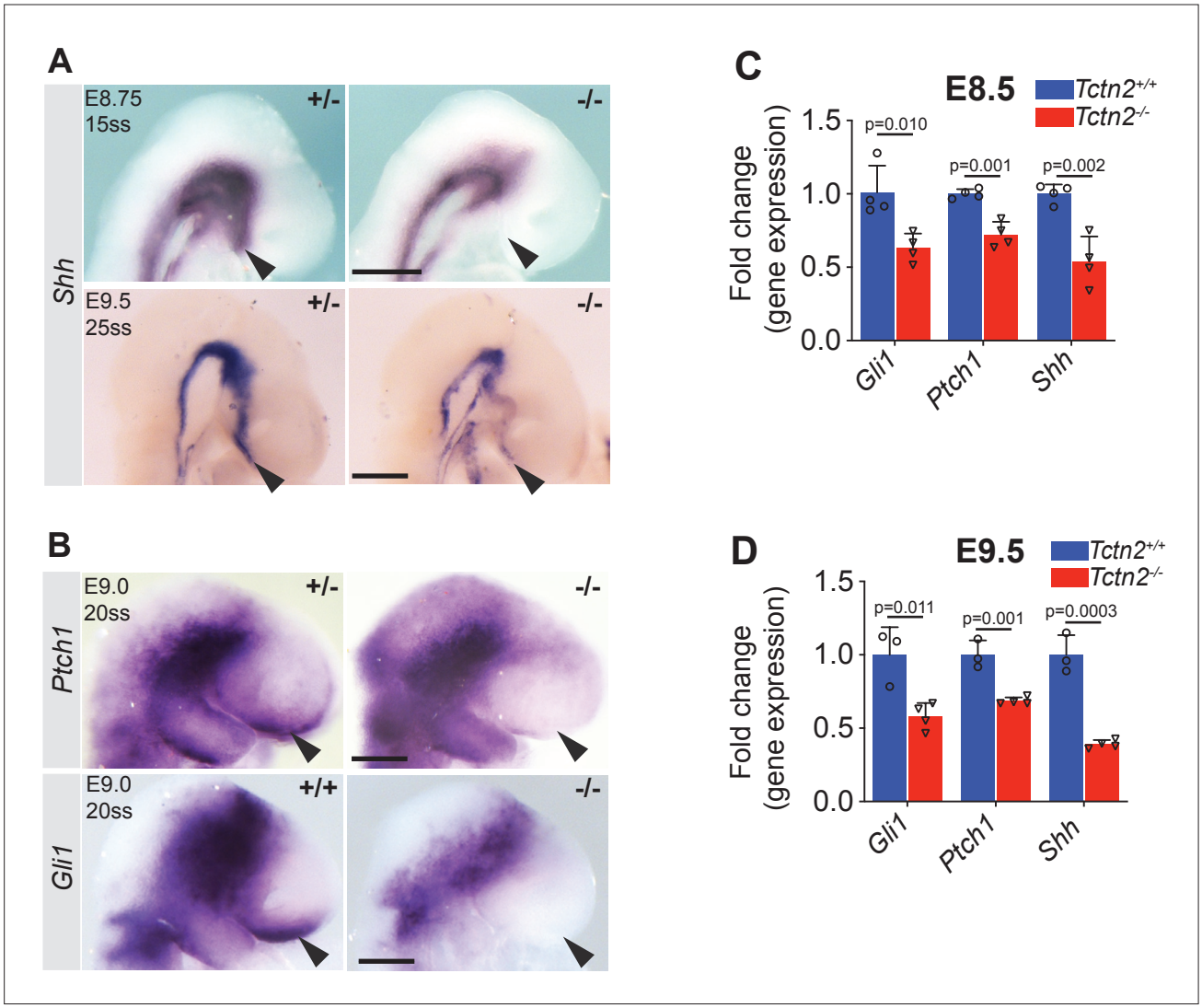

Figure 3. *Tctn2* mutants display decreased Hedgehog (HH) signaling in the ventral telencephalon. Whole mount in situ hybridization (WM-ISH) for *Shh* in *Tctn2* control and mutant embryos at embryonic day (E)8.75 and E9.5 (**A**) show reduced expression in the ventral telencephalon of mutant embryos (arrowheads). WM-ISH for HH pathway targets *Ptch1* and *Gli1* also show reduced expression in the ventral telencephalon in *Tctn2* mutants (B, arrowheads). Quantitative real-time polymerase chain reaction (RT-qPCR) analysis of RNA transcripts isolated from E8.5 and E9.5 *Tctn2* control and mutant heads (C and D, respectively) show reduced levels of *Gli1*, *Ptch1*, and *Shh* transcripts, consistent with WM-ISH results. Data in C, D represent mean, and error bar represents the standard deviation (SD). Sample size in C and D indicated with N representing biological replicates. Student's *t* test performed for statistical analysis. Scale bar indicates 0.5 mm.

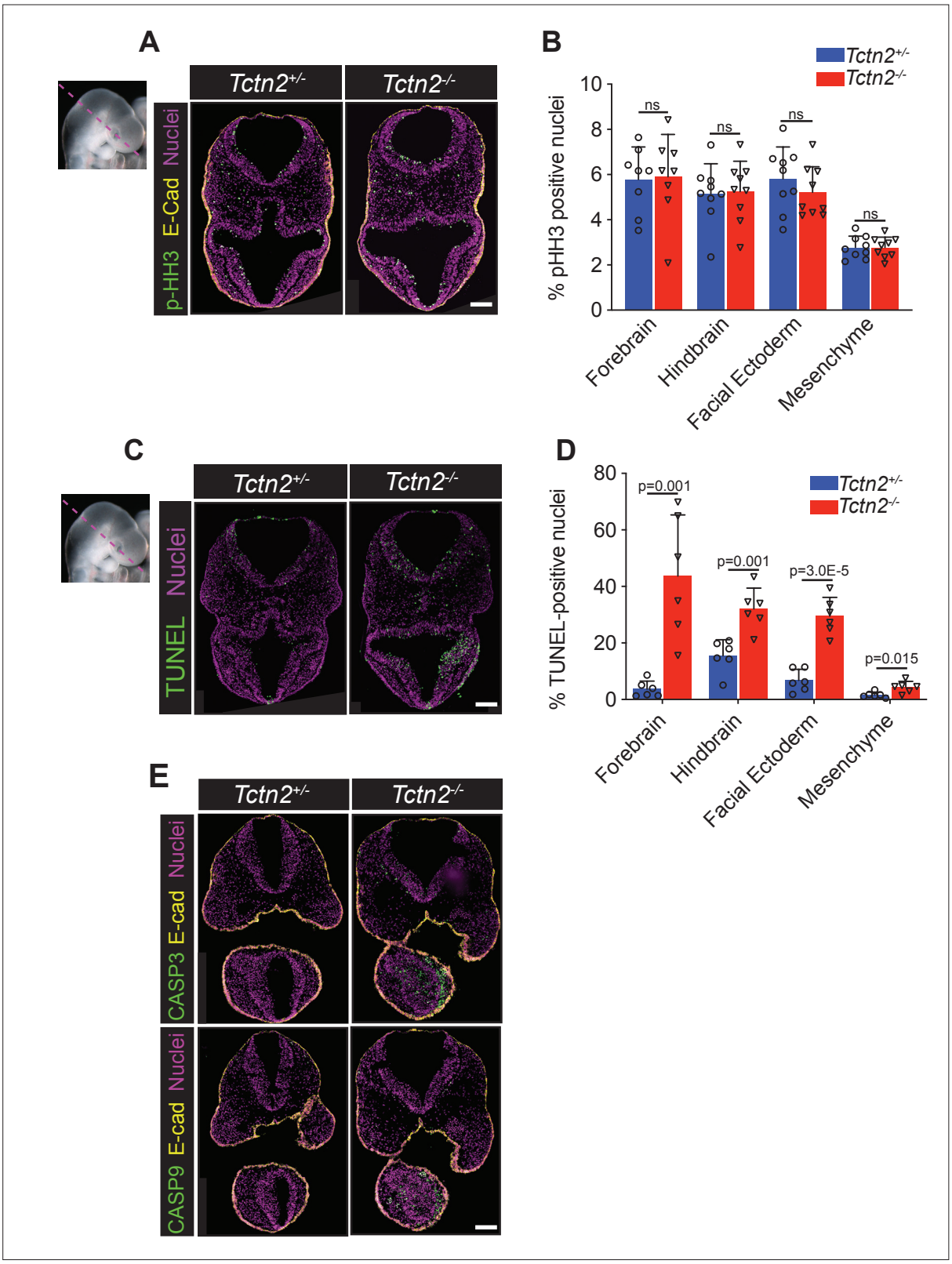

Figure 4. TCTN2 protects the neurectoderm and facial ectoderm from apoptosis. Immunostaining for proliferation marker phospho-histone H3 (pHH3) in transverse sections of *Tctn2* control and mutant embryonic day (E9.5) embryos (**A**) with corresponding quantification (**B**). (**C**) TUNEL staining for analysis of apoptosis in *Tctn2* E9.5 embryos with corresponding quantification (**D**). (**E**) Immunostaining for intrinsic apoptotic pathway components cleaved-caspase-3 and cleaved-caspase-9 in *Tctn2* control and mutant E9.5 embryos. Quantified data represent N = 3 biological replicates (biologically

Figure 4 continued on next page

Figure 4 continued

distinct samples) with a minimum of two sections analyzed per sample. Student's *t* test performed for statistical analysis. Data in B, D represent the mean, and error bars represent the standard deviation (SD). Scale bar indicates 100 μm. ns = not significant.

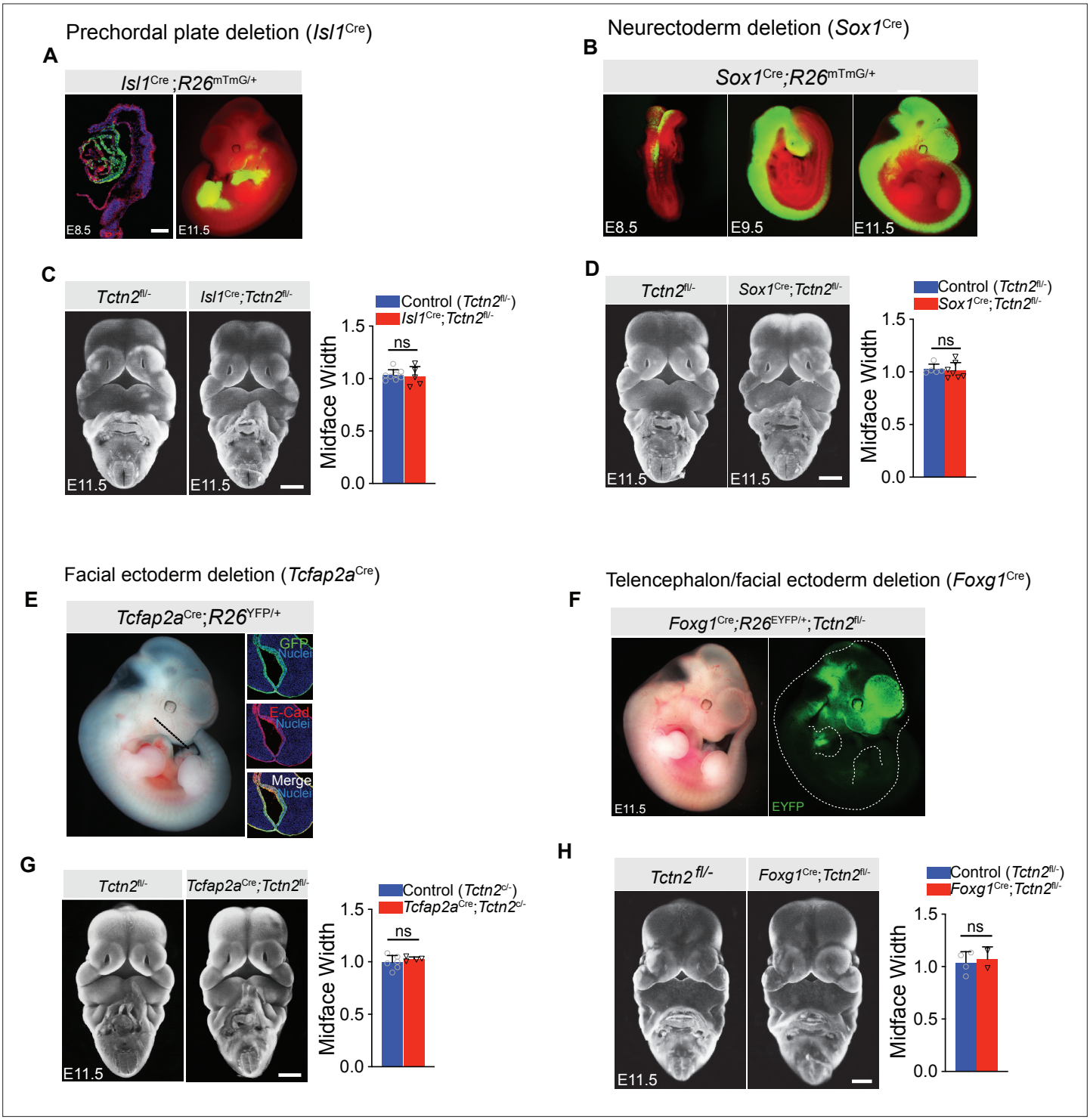

Figure 4—figure supplement 1. Deletion of *Tctn2* in the prechordal plate by *Isl1*^{Cre}, neurectoderm by *Sox1*^{Cre}, facial ectoderm by *Tcfap2a*^{Cre}, or forebrain and facial ectoderm by *Foxg1*^{Cre} does not result in hypotelorism. (**A**) Analysis of *Isl1*^{Cre} recombination pattern at E8.5 and E11.5 using the *R26*^{mTmG} reporter shows robust recombination in the prechordal plate and endodermal derivatives at respective timepoints. (**B**) Analysis of *Sox1*^{Cre} recombination pattern at E8.5, E9.5, and E11.5 using the *R26*^{mTmG} reporter shows early recombination in the neural folds at E8.5 followed by robust recombination throughout the neurectoderm at E9.5 and E11.5. (**C**) Frontal view images of E11.5 control (*Tctn2*$^{fl/-}$) and mutant (*Isl1*^{Cre};*Tctn2*$^{fl/-}$) embryos with corresponding midface width quantification. (**D**) Frontal view images of E11.5 control (*Tctn2*$^{fl/-}$) and neurectoderm-specific *Tctn2* mutant (*Sox1*^{Cre};*Tctn2*$^{fl/-}$) embryos with corresponding midface width quantification. (**E**) Analysis of *Tcfap2a*^{Cre} recombination pattern at E11.5 using the *R26*^{EYFP} reporter shows robust recombination in the facial ectoderm as evidenced by colocalization with epithelial marker E-cadherin (E-Cad). (**F**) Analysis

Figure 4—figure supplement 1 continued on next page

Figure 4—figure supplement 1 continued

of *Foxg1*^{Cre} recombination pattern at E11.5 using the *R26*^{EYFP} reporter shows expected robust recombination in the forebrain and facial ectoderm at E11.5. (**G**) Frontal view images of E11.5 control (*Tctn2*$^{fl/-}$) and facial ectoderm deletion (*Tcfap2a*^{Cre};*Tctn2*$^{fl/-}$) embryos with corresponding midface width quantification. (**H**) Frontal view images of E11.5 control (*Tctn2*$^{fl/-}$) and forebrain/facial ectoderm-specific *Tctn2* deletion (*Foxg1*^{Cre};*Tctn2*$^{fl/-}$) embryos with corresponding midface width quantification. Dotted line in E indicates approximate section through midface for immunofluorescence images in E. Dotted white line in F indicates embryo outline. Quantified data in C, D, G, and H represent the mean with error bars indicating standard deviation (SD) and each individual data point indicates a biological replicate. Student's *t* test performed for statistical analysis of C, D, G, and H. Scale bars indicate 100 μm in B, 500 μm in C, D, G, and H. ns = not significant.

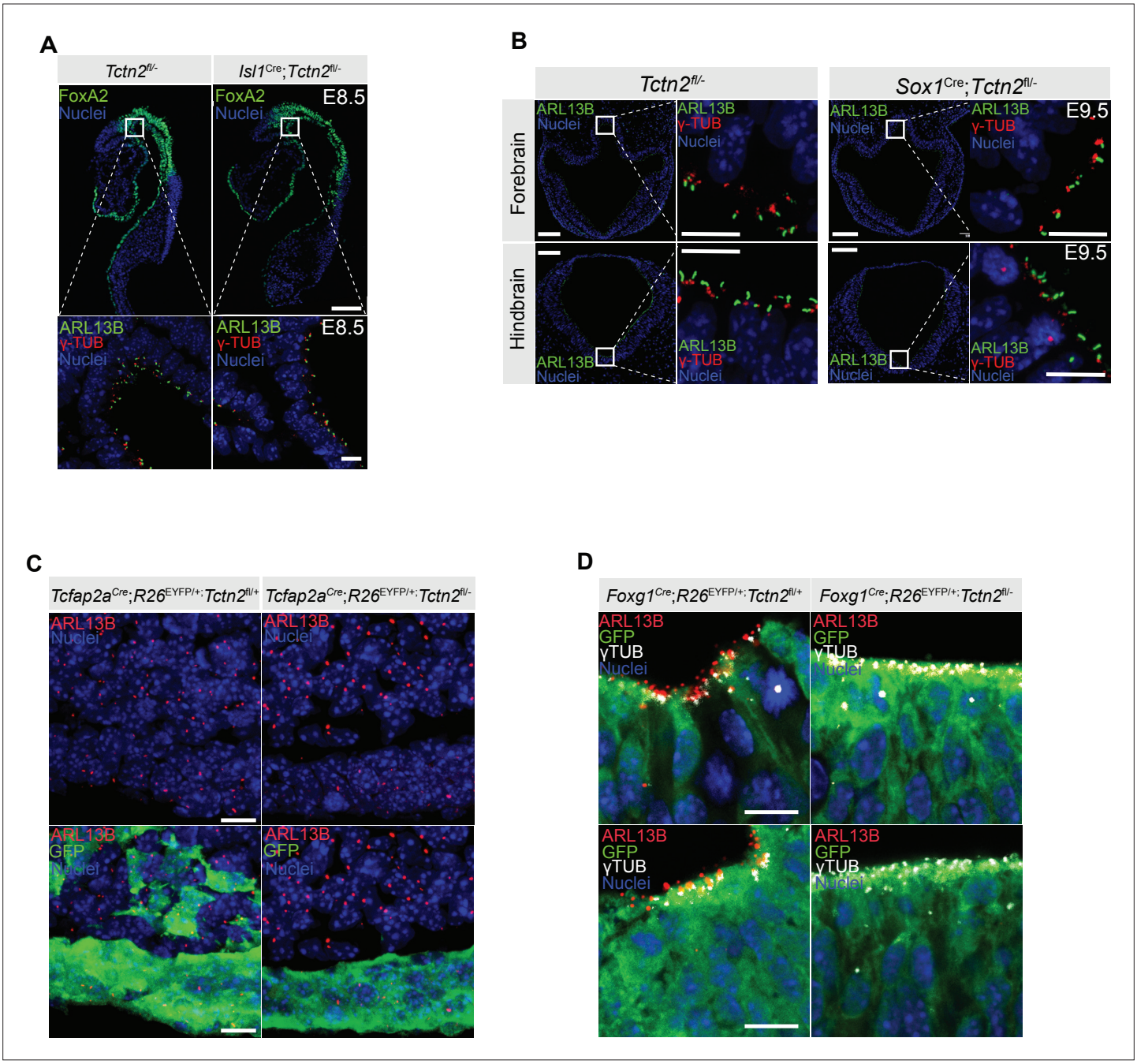

Figure 4—figure supplement 2. Residual TCTN2 function through persistent ARL13B ciliary localization in TCTN2 conditional mutants. (**A**) Analysis of *Tctn2* deletion in the prechordal plate of embryonic day (E)8.5 *Isl1*^{Cre};*Tctn2*$^{fl/-}$ embryos through ciliary localization of ARL13B indicates residual TCTN2 function remains at this early timepoint despite reporter recombination. (**B**) Analysis of *Tctn2* deletion in the neurectoderm of E9.5 *Sox1*^{Cre};*Tctn2*$^{fl/-}$ embryos through ciliary localization of ARL13B in the forebrain (top panels) and hindbrain (bottom panels) indicates residual TCTN2 function remains at this early timepoint despite robust reporter recombination.(**C**) Analysis of *Tctn2* deletion in the facial ectoderm of E11.5 *Tcfap2a*^{Cre};*Tctn2*$^{fl/-}$ embryos through ciliary localization of ARL13B indicates residual TCTN2 function remains at this timepoint as ARL13B accumulation in cilia persists in the facial ectoderm of *Tcfap2a*^{Cre};*Tctn2*$^{fl/-}$ mutants. (**D**) Immunofluorescence staining of E11.5 neural tube sections for ciliary membrane protein ARL13B, basal body marker gamma tubulin (γ TUB), and α-GFP for readout of reporter recombination shows loss of TCTN2 function in *Foxg1*^{Cre};*Tctn2*$^{fl/-}$ embryos through loss of ARL13B ciliary accumulation. Low-magnification images in A and B indicate 100 μm, and high-magnification images in A (bottom panels), B (right panels), C, and D indicate 10 μm. ns = not significant.

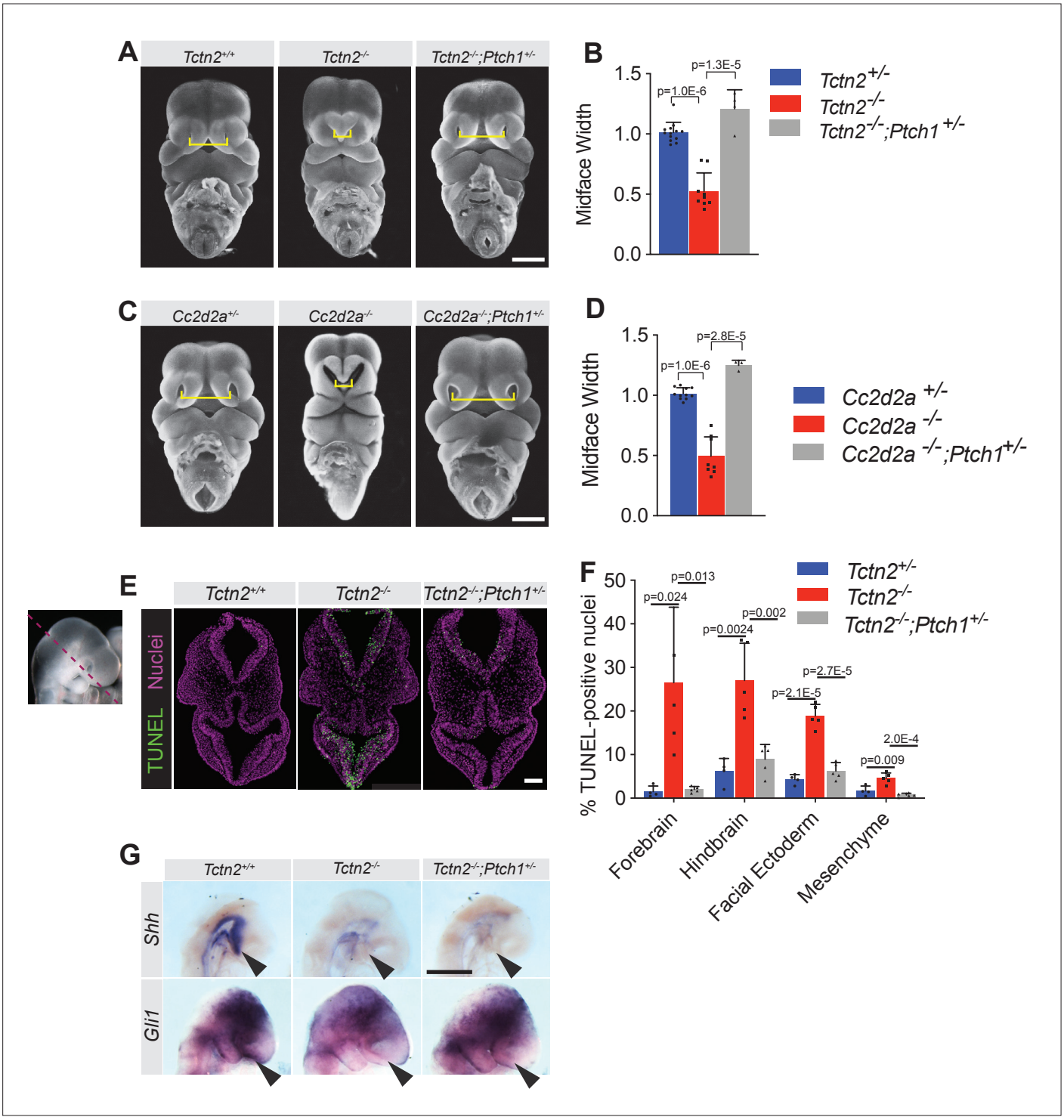

Figure 5. Reducing *Ptch1* gene dosage rescues the facial midline defect in transition zone mutants. (**A**) Frontal images of *Tctn2* wildtype, mutant, and *Ptch1*$^{+/-}$ rescue embryonic day (E)11.5 embryos with corresponding midline width quantification (**B**). (**C**) Frontal images of *Cc2d2a* wildtype, mutant, and *Ptch1*$^{+/-}$ rescue E11.5 embryos with corresponding midline width quantification (**D**). (**E**) TUNEL assay sections of E9.5 *Tctn2* wildtype, mutant, and *Ptch1*$^{+/-}$ rescue with corresponding quantification (**F**). (**G**) Whole mount in situ hybridization (WM-ISH) of E9.5 *Tctn2* wildtype, mutant, and *Ptch1*$^{+/-}$ rescue embryos for *Shh* and *Gli1*. Quantified data represent N = 3 biological replicates (biologically distinct samples) with a minimum of two sections analyzed per sample. Data in B, D, F represent the mean, and error bars represent the standard deviation (SD). For statistical analysis, one-way ANOVA was performed with Tukey's multiple comparison test. Scale bars indicate 500 µm (**A, C, G**) and 100 µm (**E**).

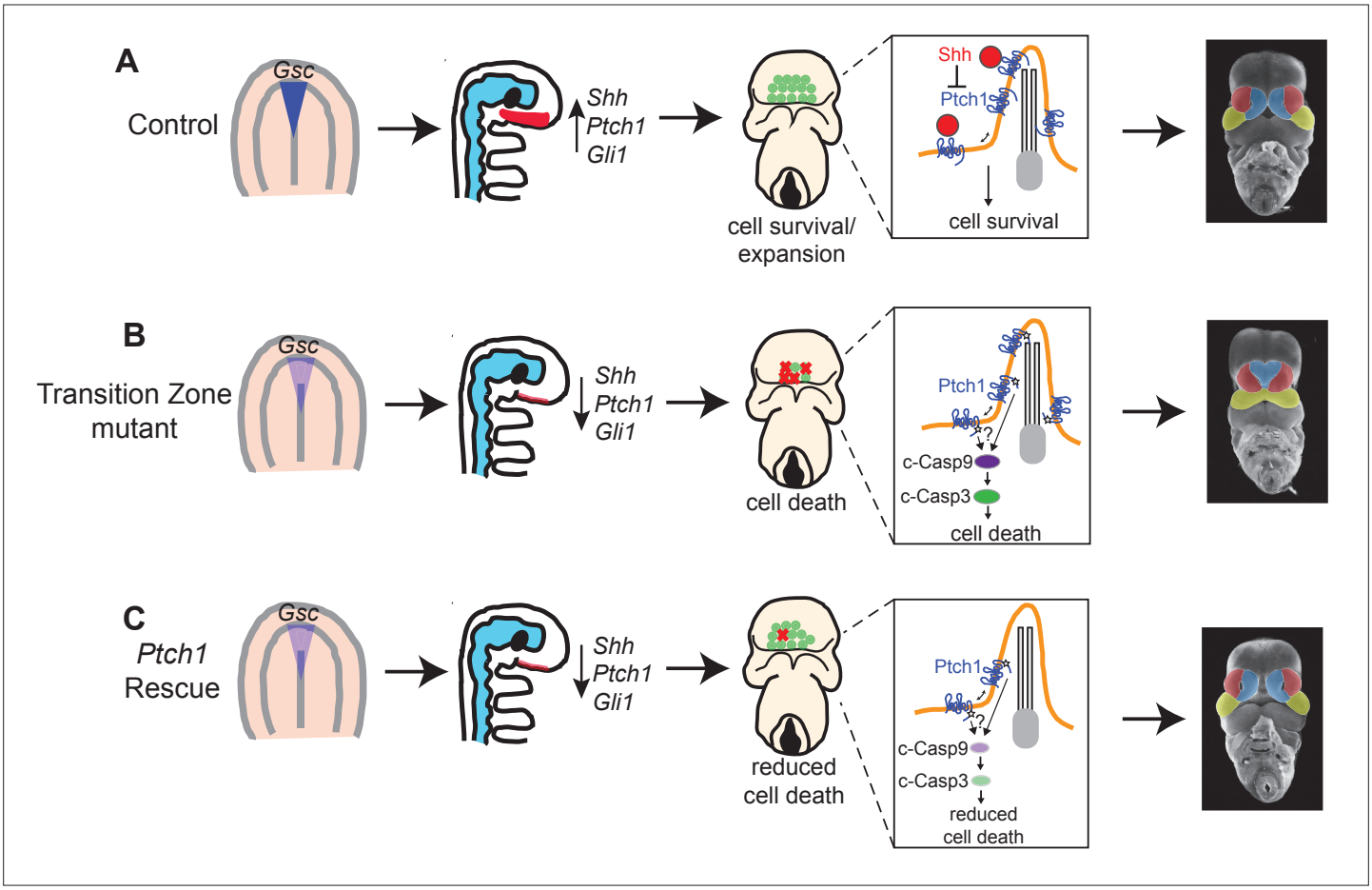

Figure 6. Model for transition zone coordination of facial midline development. (**A**) In wildtype embryos, the transition zone complex mediates signaling in the prechordal plate and Hedgehog (HH) pathway activation in the adjacent neurectoderm to at allow for cell survival and normal midline development. (**B**) In transition zone mutants, disrupted signaling in the prechordal plate results in reduced *Shh* and HH pathway activation in the neurectoderm resulting in increased cell death and corresponding collapse of the facial midline. (**C**) In TZ mutants with *Ptch1* haploinsufficiency (*Ptch1* rescue), reduced cell death allows for normal midface development despite persistent reduction of *Shh* and HH pathway activation in the neurectoderm.